

# 1D transition-metal dichalcogenides/carbon core-shell composites for Hydrogen Evolution Reaction

Asmita Dutta<sup>1</sup>, Ortal Breuer<sup>2</sup>, Manjunath Krishnappa<sup>3</sup>, Refael Minnes<sup>4</sup>, Alla Zak<sup>3</sup>, Arie Borenstein<sup>1</sup>

1- Department of Chemical Sciences, Ariel University, Israel

2- Department of Chemistry, Bar-Ilan University, Israel

3- Faculty of Sciences, Holon Institute of Technology, Israel

4- Department of Physics, Ariel University, Israel

\*- Corresponding author. Email: arieb@ariel.ac.il

## Table of Contents

### Tables

Table S1	XPS Peak Table of different elements	2
Table S2	XPS % calculation of tungsten	2
Table S3	Comparison of electrochemical performances of similar electrocatalysts	3
Table S4	Values of EIS spectra in 0.5 M H <sub>2</sub> SO <sub>4</sub>	4

### Figures

Figure S1	Low magnification STEM image	5
Figure S2	EDS of the carbon-coated WS <sub>2</sub> tube	5
Figure S3	Percentage analysis of XRD spectrum	6
Figure S4	Absolute absorption spectra	6
Figure S5	Raman spectroscopy of the WS <sub>2</sub> /C composites	7
Figure S6	Full XPS spectrum of the WS <sub>2</sub> /C composites	7
Figure S7	XPS of S2p and N1s for of the WS <sub>2</sub> /C composites	8
Figure S8	XPS of pristine WS <sub>2</sub> Peak splitting of W4f and C1s	8
Figure S9	MS results of chronoamperometry	9
Figure S9	LSVs of the Toray carbon paper	9
Figure S10	CVs of the WS <sub>2</sub> /C composites in 0.5 M H <sub>2</sub> SO <sub>4</sub>	10
Figure S11	O-WS <sub>2</sub> /C at acidic and neutral solutions.	10
Figure S12	A-WS <sub>2</sub> /C at acidic and neutral solutions.	11
Figure S13	Tafel slope in different pH solutions	11
Figure S14	CV before and after the 12 h of chronoamperometry	12

## Tables

**Table S1:** XPS Peak table for all the carbon-coated samples along with pristine WS<sub>2</sub>.

Samples	WS <sub>2</sub>	A-WS <sub>2</sub> /C	O-WS <sub>2</sub> /C	R-WS <sub>2</sub> /C
Carbon	33.18	40.21	41.74	31.85
C-C	22.48	33.64	26.15	15.85
C-O	9.35	4.84	12.52	13.55
C=O	2.19	1.88	3.86	2.01
Oxygen (O1s)	14.64	5.49	9.01	21.65
Sulphur (s2p)	11.41	7.04	2.87	6.84
Tungsten (W4f)	4.82	3.32	1.79	4.77
Nitrogen (N1s)	2.46	3.58	2.07	3.5

**Table S2:** Atomic % of WS<sub>2</sub> (4f<sub>7/2</sub>+4f<sub>5/2</sub>) and WO<sub>3</sub> (4f<sub>7/2</sub>+4f<sub>5/2</sub>) content in the catalysts compared with total atomic % of W, obtained in XPS.

Samples	Atomic % of WS <sub>2</sub> or WO <sub>2</sub> (4f <sub>7/2</sub> +4f <sub>5/2</sub> )/W	Atomic % of WO <sub>3</sub> (4f <sub>7/2</sub> +4f <sub>5/2</sub> )/W	Total atomic % of W
WS <sub>2</sub>	95	0	7.67
A-WS <sub>2</sub> /C	89	0	3.17
O-WS <sub>2</sub> /C	53.73	44.17	3.35
R-WS <sub>2</sub> /C	35.61	61.75	8.76

**Table S3:** Comparison of electrochemical performances of similar electrocatalysts

Catalysts	Current density, mA cm <sup>-2</sup>	Overpotential (mV vs. RHE)	Journal, Year of Publication	Ref.
2D graphene/WS <sub>2</sub> nanosheet	10	180	<i>ACS Appl. Energy Mater.</i> , 2021	42
WS <sub>2</sub> /C	10	179	Journal of Fuel Chemistry and Technology, 2021	43
WS <sub>2</sub> /OCF	10	278	Applied Surface Science, 2017	44
WS <sub>2</sub> /rGO	10	170	Nanoscale, 2015	45
hierarchical triple-shelled (WS <sub>2</sub> -C-WS <sub>2</sub> ) hollow nanospheres	10	175	Journal of Material Chemistry A, 2018	46
Carbon foam-N-doped Graphene-@ MoS <sub>2</sub>	10	170	Journal of Material Chemistry A, 2013	47
N-enriched C foam@WS <sub>2</sub>	10	153	Applied Surface Science, 2019	48
N,S doped graphene	10	390	Angewandte Chemie, 2014	49
N, P co-doped carbon-encapsulated CoP/MoP hybrid	10	183	Journal of Colloid and Interface Science, 2023	50
WS <sub>2</sub> Nanoribbons	10	225	Advanced Energy Materials, 2014	17
MoS <sub>2</sub> -WS <sub>2</sub>	10	129	<i>ACS Sustainable Chem. Eng.</i> , 2018	51
R-WS <sub>2</sub> /C	10	172		This work

**Table S4:** Values of resistances and capacitances from EIS spectra in 0.5 M H<sub>2</sub>SO<sub>4</sub>

	R <sub>s</sub> (Ohm)	R <sub>1</sub> (Ohm)	CPE <sub>1</sub> (μF)
WS <sub>2</sub>	3.48	56.7	6.25
Carbon	2.71	9.01	8.08
A-WS <sub>2</sub> /C	4.13	13.77	242
O-WS <sub>2</sub> /C	2.78	11.21	7605
R-WS <sub>2</sub> /C	4.8	8.87	1642

The equivalent circuit contains a resistor (R<sub>s</sub>) connected with two parallel units in series: a constant phase element and a resistor (CPE<sub>1</sub>-R<sub>ct</sub>). The R<sub>s</sub> represents the solution resistance, and the CPE<sub>1</sub>- R<sub>ct</sub> pair is equivalent to resistor and capacitor in parallel combination related to the charge transfer.

## Figures

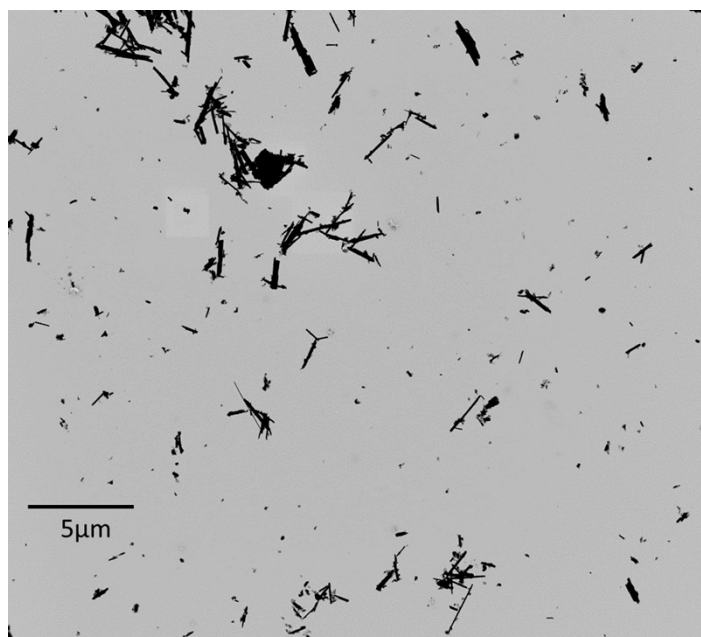


**Figure S1:** Low magnification STEM image of WS<sub>2</sub> NTs/carbon composite showing the NTs are well dispersed throughout the grid.

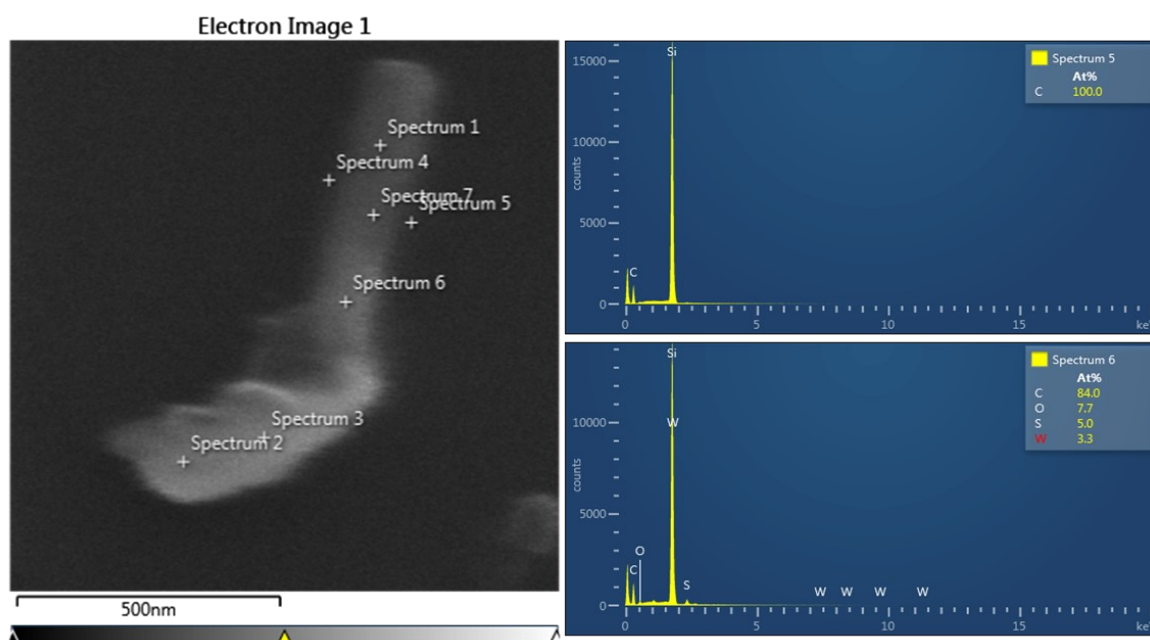


**Figure S2:** *left.* Low voltage SEM image of the carbon-coated WS<sub>2</sub> tube on silicon wafer. *Right.* EDS analysis of different points on the nanotube shown, revealing 100% carbon adjacent to the wall of the tube (point #5) as compared to elements content in the middle of the tube (point #6). The high content carbon proves that the carbon efficiently wraps all over the nanotube.

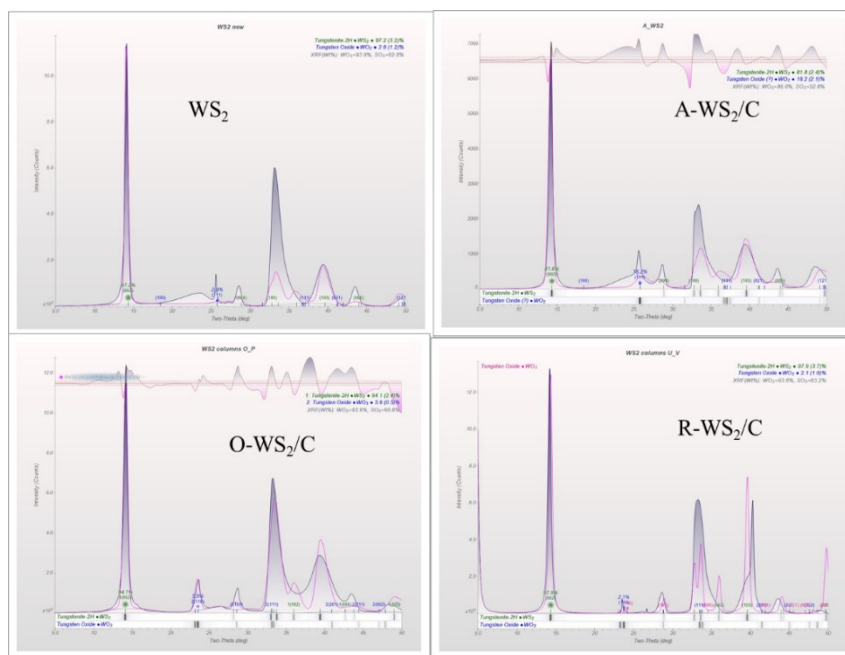
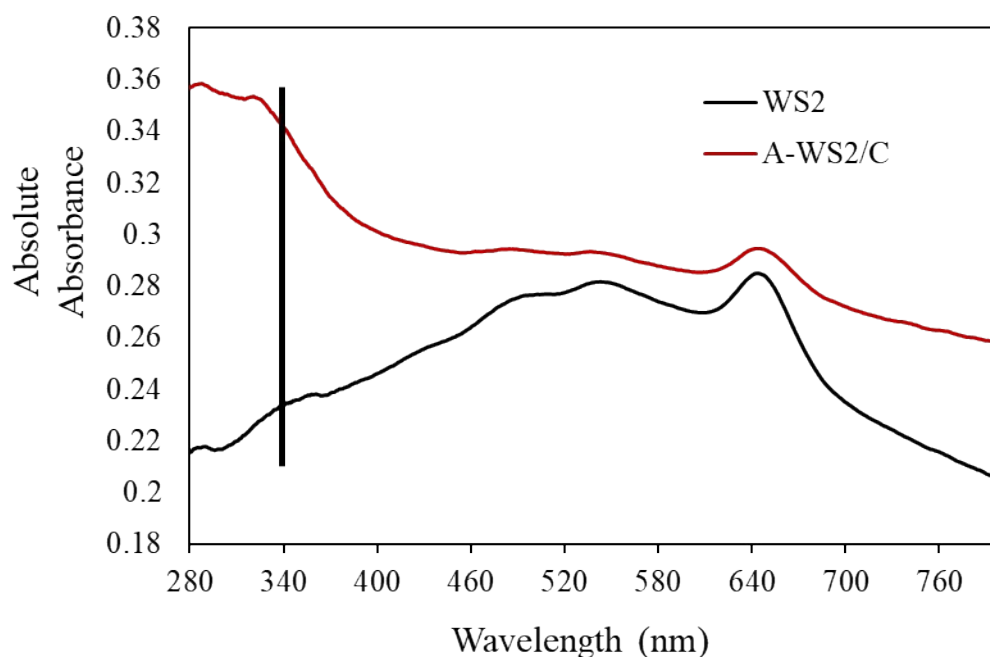
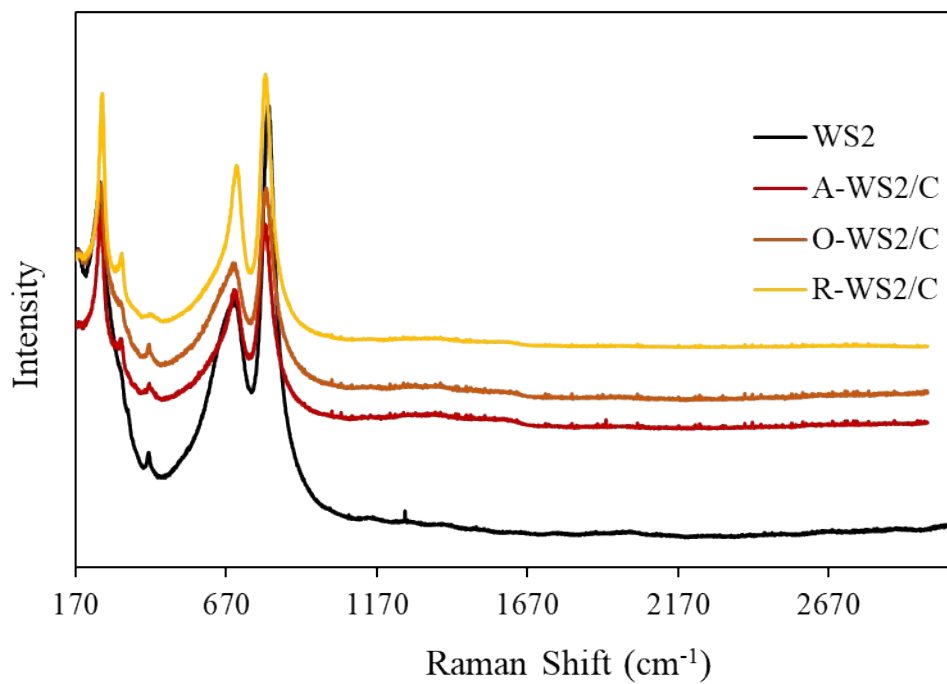


Figure S3. XRD analysis of three different samples with pristine WS<sub>2</sub> shows the presence of WO<sub>2</sub> oxide phase in pristine and first annealed (A-WS<sub>2</sub>/C) sample whereas the other two samples (O-WS<sub>2</sub>/C AND R-WS<sub>2</sub>/C) contain WO<sub>3</sub> phase. Importantly, for every sample WS<sub>2</sub> (002) peak at 2 $\theta$ =14.5 remains a higher percentage proving the unharmed crystallinity.



**Figure S4:** Absolute absorption spectra of prepared A-WS<sub>2</sub>/C showing no shift at the exciton of the nanotube. An additional peak near 340 nm appears due to the attachment of carbon with the nanotube.



**Figure S5:** Raman spectroscopy of the WS<sub>2</sub>/C composites.

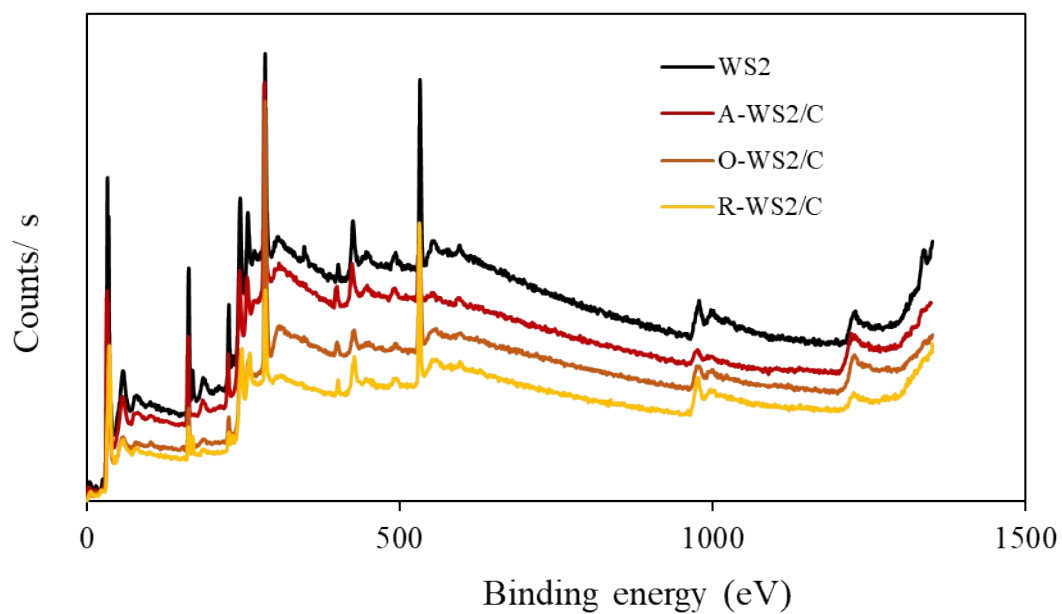


**Figure S6:** Full XPS spectrum of the WS<sub>2</sub>, A-WS<sub>2</sub>/C, O-WS<sub>2</sub>/C, R-WS<sub>2</sub>/C.

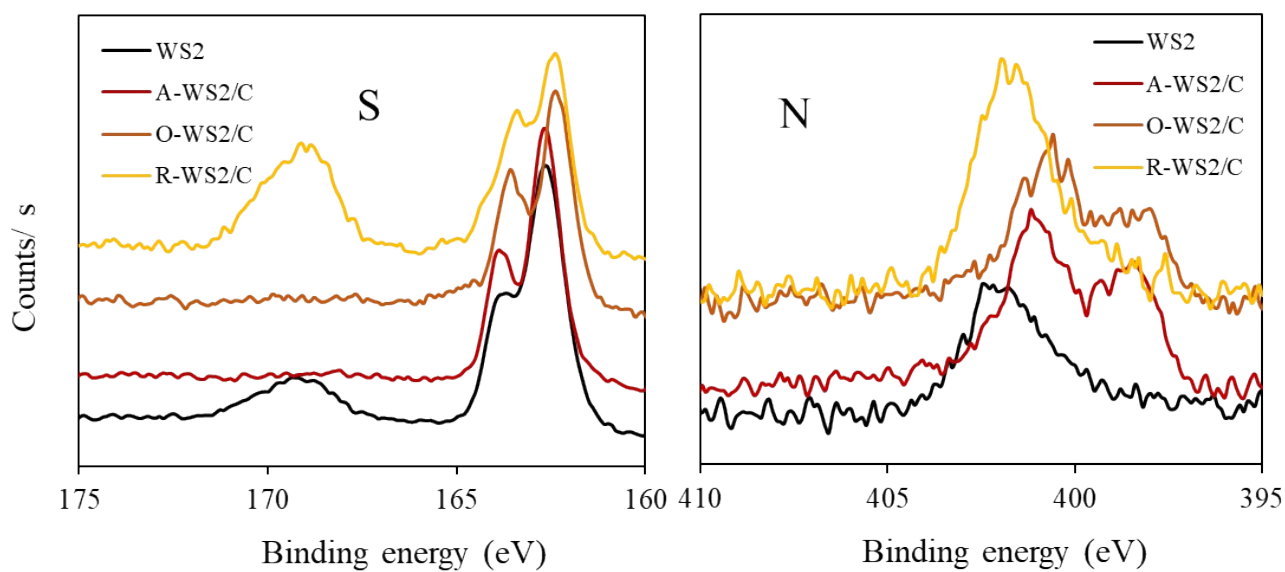


**Figure S7:** XPS of S<sub>2p</sub> and N<sub>1s</sub> for all samples.

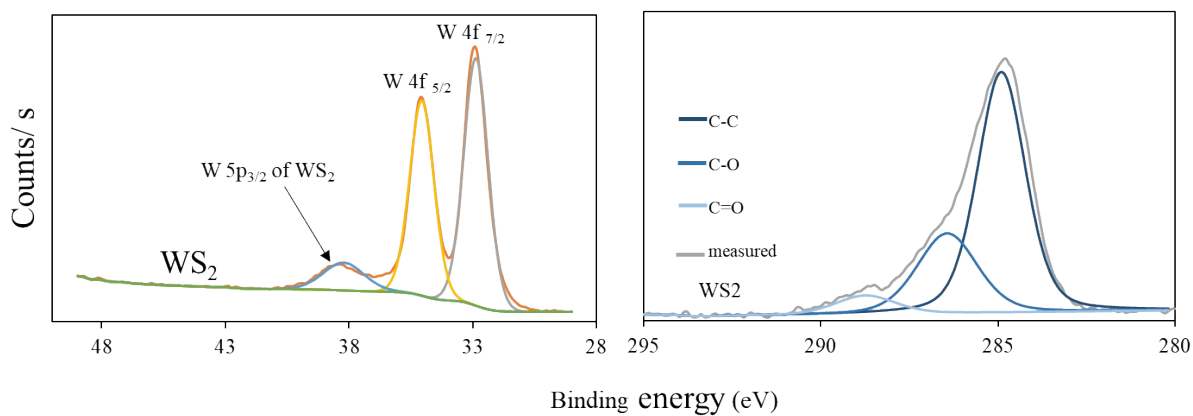


**Figure S8:** XPS spectrum of pristine WS<sub>2</sub> after peak splitting of W<sub>4f</sub> and C<sub>1s</sub> scan.

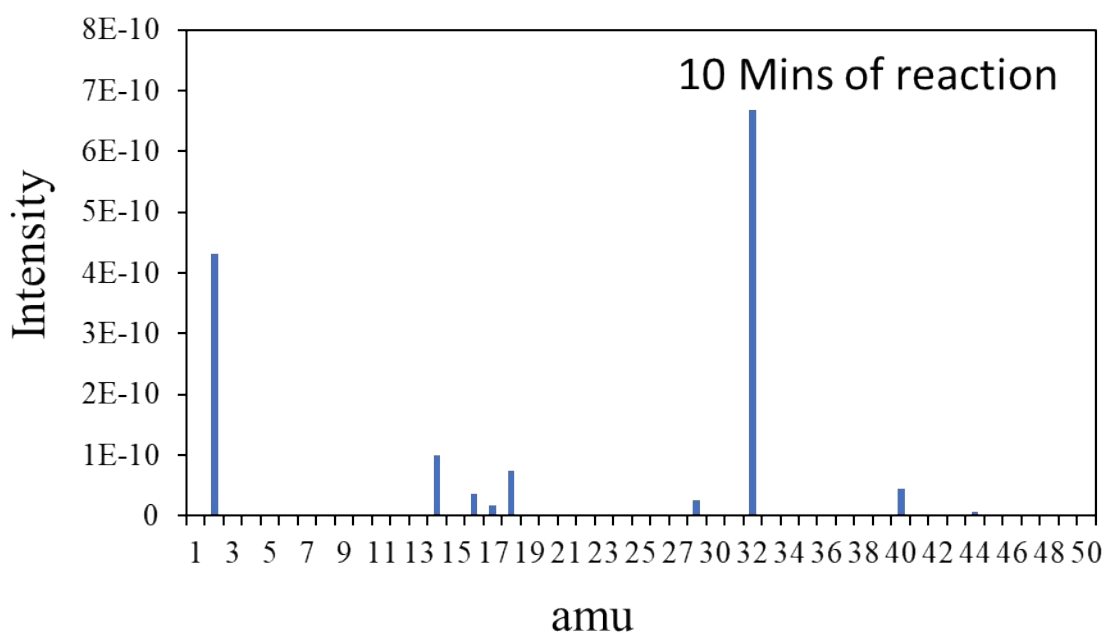


**Figure S9.** Mass spectroscopy (MS) was collected from A-WS2/C after 10 minutes of CA at its overpotential, confirming hydrogen production.

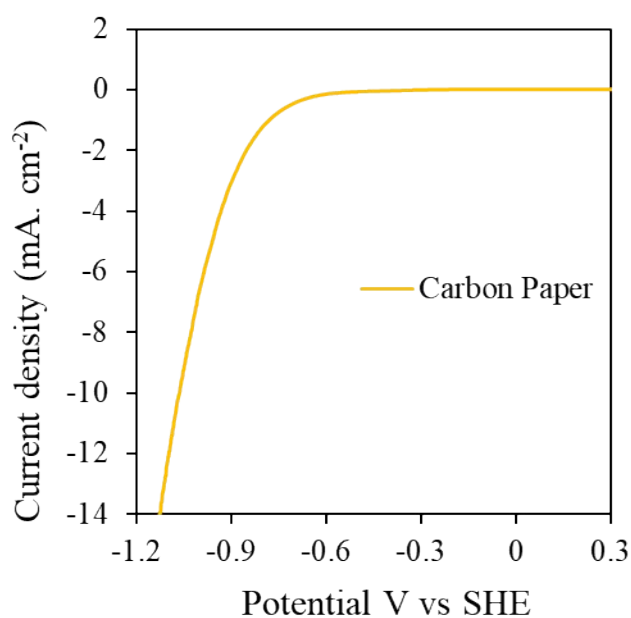


**Figure S10:** LSVs of the Toray carbon paper showing a negligible effect on the catalytic performance.

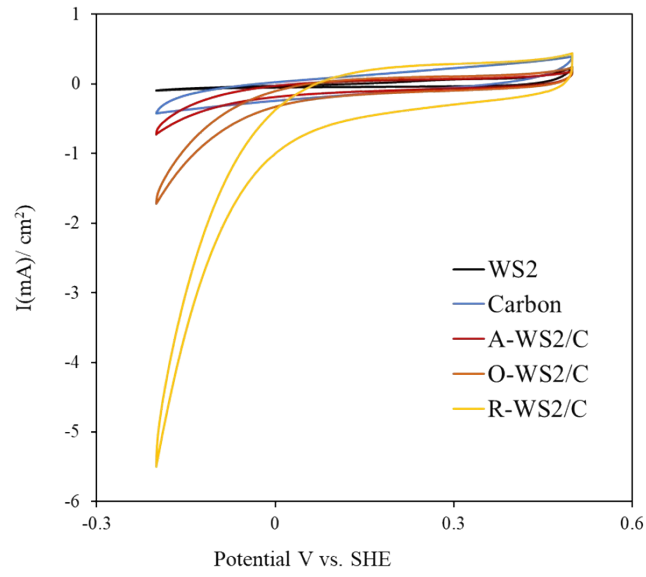


**Figure S11:** CV for all the samples in 0.5 M H<sub>2</sub>SO<sub>4</sub>.

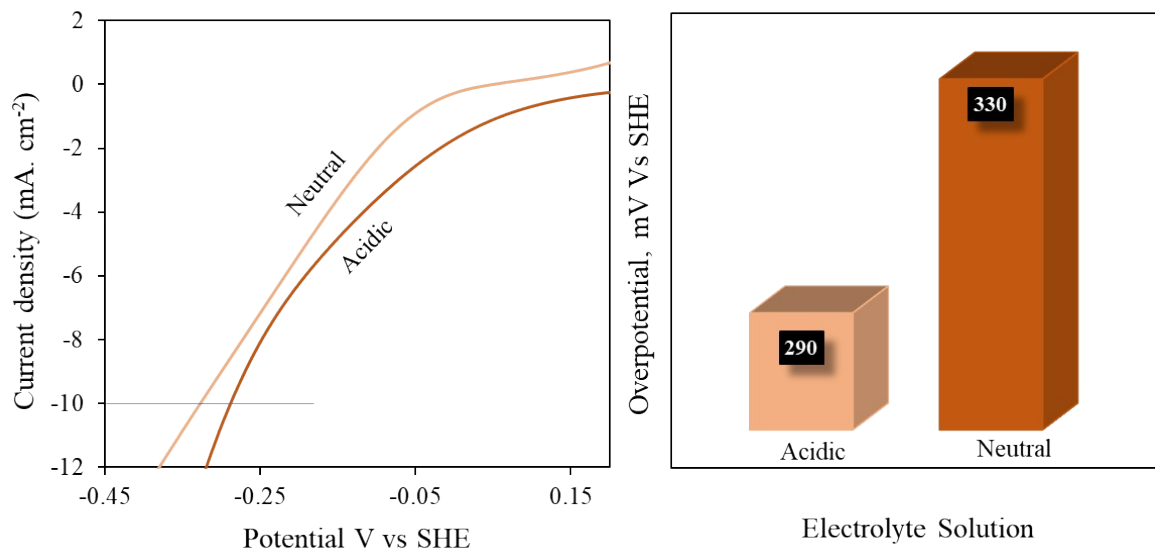


**Figure S12:** Onset potential at a current density of  $-10 \text{ mAcm}^{-2}$  of O-WS<sub>2</sub>/C at acidic and neutral solutions.

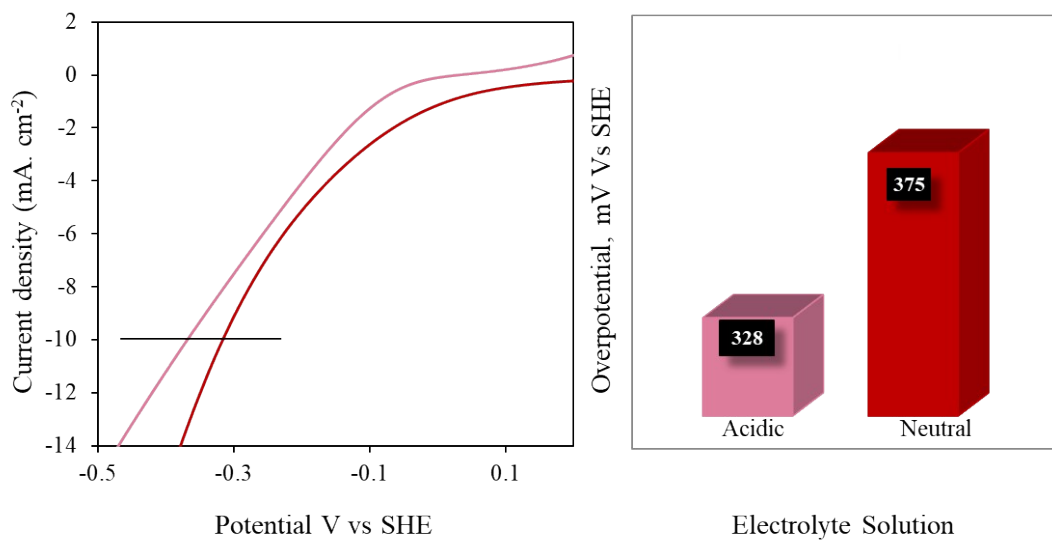


**Figure S13:** Onset potential at a current density of  $-10 \text{ mA cm}^{-2}$  of A-WS<sub>2</sub>/C at acidic and neutral solutions

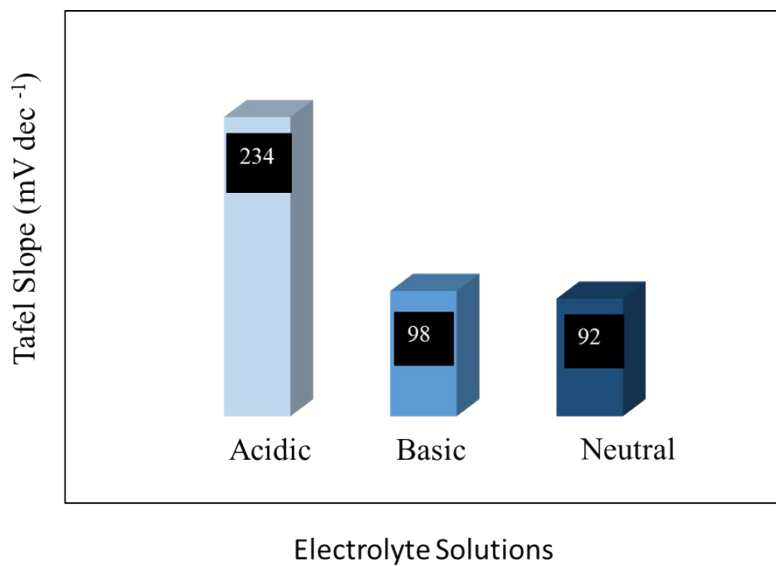


**Figure S14:** Tafel slope in different pH solutions.

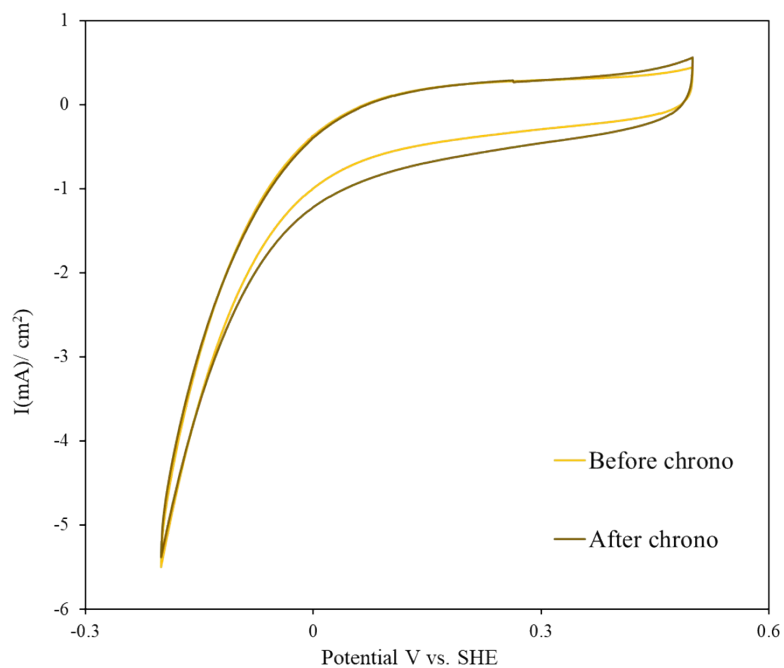


**Figure S15:** CV before and after the 12 h of chronoamperometry test with an applied voltage of -0.150V vs. RHE for the prepared WS<sub>2</sub>/C catalyst indicates that the catalyst is stable even after a long duration of hydrogen production.